A highly sensitive method for analysis of 7-dehydrocholesterol for the study of Smith-Lemli-Opitz syndrome[s]

Wei Liu,* Libin Xu,* Connor Lamberson,* Dorothea Haas,[†] Zeljka Korade,[§] and Ned A. Porter[1],*

Department of Chemistry, Vanderbilt Institute of Chemical Biology,* Department of Psychiatry, Vanderbilt Kennedy Center for Research on Human Development,[§] Vanderbilt University, Nashville, TN 37235; and Division of Inborn Metabolic Diseases,[†] University Children's Hospital, D-69120 Heidelberg, Germany

Abstract We describe a highly sensitive method for the detection of 7-dehydrocholesterol (7-DHC), the biosynthetic precursor of cholesterol, based on its reactivity with 4-phenyl-1,2,4-triazoline-3,5-dione (PTAD) in a Diels-Alder cycloaddition reaction. Samples of biological tissues and fluids with added deuterium-labeled internal standards were derivatized with PTAD and analyzed by LC-MS. This protocol permits fast processing of samples, short chromatography times, and high sensitivity. We applied this method to the analysis of cells, blood, and tissues from several sources, including human plasma. Another innovative aspect of this study is that it provides a reliable and highly reproducible measurement of 7-DHC in 7-dehydrocholesterol reductase (*Dhcr7*)-HET mouse (a model for Smith-Lemli-Opitz syndrome) samples, showing regional differences in the brain tissue. We found that the levels of 7-DHC are consistently higher in *Dhcr7*-HET mice than in controls, with the spinal cord and peripheral nerve showing the biggest differences. In addition to 7-DHC, sensitive analysis of desmosterol in tissues and blood was also accomplished with this PTAD method by assaying adducts formed from the PTAD "ene" reaction. The method reported here may provide a highly sensitive and high throughput way to identify at-risk populations having errors in cholesterol biosynthesis.—Liu, W., L. Xu, C. Lamberson, D. Haas, Z. Korade, and N. A. Porter. **A highly sensitive method for analysis of 7-dehydrocholesterol for the study of Smith-Lemli-Opitz syndrome.** *J. Lipid Res.* 2014. **55:** 329–337.

Supplementary key words desmosterol • Diels-Alder cycloaddition • PTAD • liquid chromatography-mass spectrometry • gas chromatography • 7-dehydrocholesterol reductase

Cholesterol is a multipurpose molecule serving as a structural component of cell membranes, a precursor for steroid hormones, a cofactor for signaling, and a protein-binding molecule (1, 2). The brain has the highest content of cholesterol compared with other organs and almost all of it is produced locally in the brain (3). The complex cholesterol biosynthesis pathway involves over 20 dedicated enzymes and complex cellular mechanisms of intracellular sorting and transport. Not surprisingly, errors in the cholesterol biosynthesis pathway have devastating effects on cellular structure and function (4). Mutations in one of the reductase enzymes of the cholesterol biosynthesis pathway, 7-dehydrocholesterol reductase (DHCR7) (see **Scheme 1**), leads to the accumulation of the biosynthetic intermediate 7-dehydrocholesterol (7-DHC) and this error in biosynthesis is associated with the human disorder known as Smith-Lemli-Opitz syndrome (SLOS) (5–9). Defects in another reductase enzyme, DHCR24, leads to elevated levels of desmosterol (Des) and the corresponding condition known as desmosterolosis (10).

Among the disorders known to have errors in cholesterol biosynthesis, SLOS is unique in that it results in the accumulation of the highly oxidizable 7-DHC. Indeed, 7-DHC has been found to have extreme reactivity in free radical chain peroxidation, its rate constant for oxidation being some 200 times that of cholesterol (11). Peroxidation of 7-DHC gives rise to over a dozen oxysterols in vitro and in vivo (12–15), many of which have been shown to have potent biological activities (16, 17), and some of the pathology of SLOS is likely associated with the formation of these oxysterols. SLOS, however, is not the only disorder

---

Scheme 1. Steps in cholesterol biosynthesis that utilize the reductase enzymes, DHCR24 and DHCR7.

that leads to increased levels of 7-DHC. Recent studies show that 7-DHC is greatly increased with the use of some psychiatric medications and it seems likely that exposure to other pharmaceutical or environmental agents will cause elevated levels of 7-DHC (18, 19).

We describe here a derivatization strategy for the analysis of 7-DHC that makes use of the reactive dienophilic and enophilic compound 4-phenyl-1,2,4-triazoline-3,5-dione (PTAD). PTAD reacts with conjugated dienes by a Diels-Alder reaction as shown in **Scheme 2**, a transformation that has been used as a basis of assays for vitamin D_3 (20). Isolated alkenes react with PTAD by the ene reaction (21–25), also shown in Scheme 2, and this transformation converts Des to products that can be readily assayed by HPLC-MS. The protocol reported here readily detects 7-DHC and Des in the plasma of control populations as well as in WT tissues and cell cultures.

MATERIALS AND METHODS

Materials

Unless otherwise noted, all chemicals were purchased from Sigma-Aldrich (St. Louis, MO). HPLC grade solvents were purchased from Thermo Fisher Scientific Inc. (Waltham, MA) The [25,26,26,26,27,27,27-d_7]-7-DHC (d_7-7-DHC) and -8-DHC were obtained by chemical synthesis as previously described (14, 26). The DHCR7 inhibitor AY9944 (27) was obtained from the Chemical Synthesis Core of the Vanderbilt Institute of Chemical Biology.
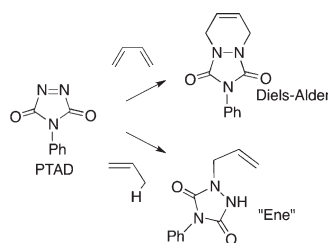
Scheme 2. Diels-Alder and ene reactions of PTAD.

Cell cultures

The neuroblastoma cell line, Neuro2a, was purchased from American Type Culture Collection (Rockville, MD). *Dhcr7*-deficient Neuro2a cells were generated as previously described (28). The cell lines were maintained in DMEM supplemented with L-glutamine, 10% fetal bovine serum (FBS) (Thermo Scientific HyClone, Logan, UT), and penicillin/streptomycin at 37°C and 5% CO_2. All cells were subcultured once a week, and the culture medium was changed every 2 days. For AY9944 treatment, Neuro2a cells were plated at $5 \times 10^4/cm^2$ in DMEM with 10% FBS. The following day the medium was replaced with serum-free medium (DMEM plus N2 supplement) with or without AY9944 (concentrations shown in Table 2) for 48 h. Cholesterol and 7-DHC were measured in cells grown for 48 h in cholesterol-deficient serum (Thermo Scientific HyClone lipid reduced FBS). The harvested cells were washed with cold PBS (pH 7.4) and centrifuged at 1,000 rpm for 10 min at 4°C. Cell pellets were stored at −80°C until further processing.

Frozen cell pellets were homogenized in RIPA lysis buffer (200 μl) in the presence of 10 μg/ml butylated hydroxytoluene (BHT) and 25 μg/ml triphenylphosphine (TPP) for each plate. After protein measurement using Bio-Rad DC Protein Assay kit, the rest of the sample (185 μl) was added to 2 ml of Folch solution (chloroform/methanol (MeOH) , 2:1, v/v) containing 0.25 mg/ml TPP, 0.005% BHT, and d_7-7-DHC (25.8 ng) as an internal standard, followed by the addition of 1 ml of 0.9% NaCl. The sample was then vigorously vortexed and centrifuged. The lower organic phase was recovered, dried under nitrogen, and then used for PTAD derivatization as described below.

Mice

Dhcr7-HET (*Dhcr7*$^{tm1Gst/J}$) mice were purchased from Jackson Laboratories (catalog # 007453). The mice were kept and bred in Division of Animal Care facilities at Vanderbilt University. For genotyping, the genomic DNA from mouse tails was extracted using the REDExtract-N-Amp tissue PCR kit (Sigma-Aldrich). Genotyping was performed using the following PCR primers: forward, ggatcttctgagggcagcctt; reverse, tctgaacccttggctgatca; neo, ctagaccgcggctagagaat. All procedures were performed in accordance with the Guide for the Humane Use and Care of Laboratory Animals. The Institutional Animal Care and Use Committee of Vanderbilt University approved the use of mice in this study.

Mouse dissection and processing of samples

WT and *Dhcr7*-HET mice were collected for the analysis of P60 (2 months of age, adult). Whole blood was obtained from the trunk after decapitation. From the same mouse the following organs were obtained: liver, retina, peripheral nerve, optic nerve, spinal cord, and the brain. The brain was separated into halves by cutting it along the median sulcus. One-half was used for dissecting specific brain regions (cortex, cerebellum, midbrain/brainstem, hippocampus, olfactory bulb, and striatum) and one-half was used as whole so that all structures were present. The wet weight of different tissues was measured and recorded. All blood and tissue samples were frozen on dry ice and stored at −80°C until further processing.

The blood (10 μl) was added to 2 ml of Folch solution containing 0.25 mg/ml TPP, 0.005% BHT, and d_7-7-DHC (25.8 ng) as the internal standard, followed by the addition of 1 ml of 0.9% NaCl. The resulting mixture was vortexed and centrifuged. The lower organic phase was recovered, dried under a stream of nitrogen, and then used for PTAD derivatization as described below. For tissue samples, 5 ml of ice-cold Folch solution containing 0.25 mg/ml TPP, 0.005% BHT, and d_7-7-DHC (258 ng) as the internal standard were added and homogenized with a blade

homogenizer (POLYTRON system PT 1200 E; Kinematica AG, Switzerland) on ice for 0.5 min. After addition of 2 ml of 0.9% NaCl, the sample was then vigorously vortexed and centrifuged. Two hundred microliters of the lower organic phase was removed, dried under nitrogen, and then used for PTAD derivatization as described below. For subset of samples, frozen tissue was homogenized in the lysis buffer (125 mM NaCl, HEPES, NP40) in the presence of BHT and TPP. After protein measurement using the Bio-Rad DC protein assay kit, the rest of the sample was used for lipid extraction as described in the Materials and Methods section on Cell cultures. For all measurements, three samples in a group were used. The statistical significance was measured using a two-tailed t-test in Microsoft Excel 2007.

Human plasma collection

Human blood taken in EDTA-coated tubes was wrapped with aluminum foil to minimize exposure to room light and was processed in a timely manner after the addition of a standard solution of BHT and TPP (10 mg BHT and 25 mg TPP in 10 ml of ethanol; 50 μl/ml plasma). All plasma samples analyzed in this study were stored at $-80°$C and shipped on dry ice. The plasma sample (10 μl) was then added to Folch solution and processed in the same way as described above for the mouse blood samples. Sample collection for this study was approved by the ethics committee of the medical faculty of the University of Heidelberg, Germany (S-071/2012).

PTAD derivatization

For protocol development, the derivatization reagent, PTAD, was dissolved in different solutions (MeOH, methylene dichloride, and Folch solution) and samples were incubated at different temperatures ($-80°$C, $0°$C, and room temperature) at various incubation times. The best results were obtained using freshly prepared solution of PTAD in MeOH; the reaction was fully completed after 30 min at room temperature. Our preferred experimental protocol was as follows: 200 μl of 1 mg/ml freshly prepared PTAD solution in MeOH was added to the residues of cell and tissue extracts acquired as described above, the solutions were let stand at room temperature with occasional shaking for 30 min, and then transferred into sample vials. The samples were stored at $-80°$C until analyzed by LC-MS/MS.

Sensitivity, stability, and repeatability of PTAD derivatization

To evaluate the sensitivity for MS detection of 7-DHC and Des before and after PTAD derivatization, limits of detection (LODs) and limits of quantitation for 7-DHC and Des with and without PTAD derivatization were determined by LC-MS/MS. The LOD was defined as a signal-to-noise ratio of 3 and the limit of quantitation was defined as a signal-to-noise ratio of 10.

The stability of PTAD derivatized sample mixtures (350 ng of Des, 45 ng of 7-DHC, and 25 ng of d_7-7-DHC as internal standard for PTAD incubations) was evaluated by analyzing the sample (stored at room temperature) for 4 weeks. The intra-vial repeatability of PTAD derivatization was determined by repeated analysis (n = 3) of the same sample (350 ng of Des, 45 ng of 7-DHC, and 25 ng of d_7-7-DHC as internal standard for PTAD incubations). The repeatability of PTAD derivatization for inter-vial comparisons was determined by measuring the samples of derivatization incubated in different vials under similar conditions (n = 3), described above for 7-DHC derivatization.

LC-MS/MS conditions and data analysis

LC separations were performed on a Waters Acquity UPLC system equipped with an autosampler (Waters, Milford, MA) using a Waters Acquity UPLC BEH C18 column (1.7 μm, 2.1 × 100 mm).

The injection volume was 10 μl using a partial loop with needle overfill mode. MS detections were done using a TSQ Quantum Ultra tandem mass spectrometer (ThermoFisher), and data was acquired using a Finnigan Xcalibur software package.

Analyses of PTAD derivatized samples were carried out with an isocratic solvent of MeOH/HOAc (100:0.1, v/v) at a flow rate of 0.3 ml/min. Column life was not affected by the protocol and separations were unchanged after 1,500 injections. MS/MS analysis of the 7-DHC-PTAD derivative was acquired in the positive ion mode using atmospheric pressure chemical ionization (APCI) and selected reaction monitoring (SRM). MS parameters were optimized for 7-DHC-PTAD and were as follows: auxiliary gas pressure was set at 55 psi and sheath gas pressure was 60 psi, nitrogen was utilized for both. The discharge current was set at 22 μA and the vaporizer temperature was set at 265°C. Collision induced dissociation (CID) was optimized at 12 eV under 1.0 mTorr of argon.

For the detection of 7-DHC without derivatization, the LC separation was performed with an isocratic solvent of ACN/MeOH/HOAc (50:50:0.1, v/v/v) at a flow rate of 0.3 ml/min. MS/MS analysis was performed using APCI source in the positive ion mode. SRM was used for LOD determination. MS parameters optimized for 7-DHC were as follows: auxiliary gas pressure was set at 15 psi and sheath gas pressure was 30 psi, nitrogen was utilized for both. The discharge current was set at 12 μA and the vaporizer temperature was set at 300°C. CID was optimized at 16 eV under 1.0 mTorr of argon.

Free sterol analysis by GC

For GC analysis of free sterol, the sample was processed in a similar way to the above procedure for lipid extraction, but using 5β-cholestan-3α-ol as the internal standard. Extracts were dried under nitrogen, converted to trimethylsilyl ether derivatives that were analyzed by GC, which was performed using a Hewlett-Packard HP6890 GC instrument equipped with a SPB-5 column (30 m, 0.32 mm i.d., 250 μm film thickness; Supelco, Sigma-Aldrich) and a FID. The injector was set at 220°C, and the following gradient was used: 220°C for 1 min, followed by 15°C/min up to 250°C, 1°C/min up to 275°C, and 275°C for 5 min.

RESULTS

Formation and properties of PTAD-sterol adducts

The reaction of 7-DHC with PTAD occurs readily at room temperature in nearly quantitative yield and the cycloadduct, 7-DHC-PTAD (shown in **Fig. 1**), is stable at room temperature for extended periods of time (>4 weeks). The 7-DHC-PTAD compound chromatographs well on normal or reverse-phase HPLC and it gives a strong signal at $m/z =$ 560 Da for the protonated molecular species in positive ion APCI-MS. CID of the $m/z = 560$ Da ion gives a major fragment corresponding to the loss of PTAD and water at $m/z = 365$ Da.

Our initial approach for the analysis of biological samples was to extract lipids by the Folch method in the presence of a known quantity of d_7-7-DHC, followed by addition of an excess amount of PTAD in methylene chloride or chloroform. While this method works well on a 7-DHC standard, HPLC-MS/MS analyses of biological samples using this approach were complicated by the fact that other sterols, such as cholesterol, 8-DHC, and Des, also react with PTAD. The complex set of products from cholesterol,
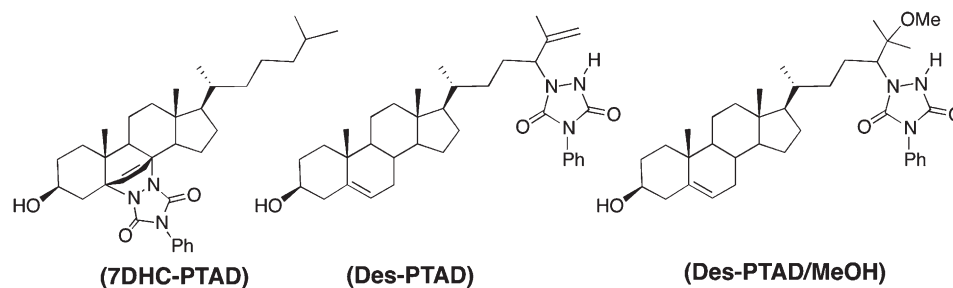
Fig. 1. Structure of 7-DHC and Des-PTAD products.

which is usually the major sterol present in biological samples, elute on HPLC at retention times close to that of 7-DHC-PTAD, making rapid HPLC-MS/MS analysis of 7-DHC-PTAD very difficult.

To overcome this problem, we tested the PTAD reaction using 7-DHC, cholesterol, Des, and 8-DHC as substrates. A screen of different reaction solvents (CH_2Cl_2, MeOH, and Folch solution), temperatures ($-80°C$, $0°C$, and room temperature), and reaction durations showed that addition of excess PTAD gave the stable adduct of 7-DHC quantitatively within 5 min at $0°C$ in all solvents. Cholesterol-PTAD ene products (Scheme 2) began to form in CH_2Cl_2 after 10 min incubation at room temperature, but MeOH suppressed the formation of this adduct. Thus, to avoid complications from cholesterol-PTAD adducts in the assay of 7-DHC, we chose the reaction in MeOH at room temperature for 30 min as the preferred PTAD protocol.

Under our MeOH PTAD protocol Des was converted nearly quantitatively to two products that separated from 7-DHC-PTAD under most HPLC conditions. These Des products could be separated by HPLC and they were characterized as the ene and solvent addition products of Des (21–24, 29) shown in Fig. 1.

7-DHC-PTAD assays in human plasma

Human plasma contains approximately 0.01 mg/dl of free (nonesterified) 7-DHC (30, 31), a very low level that is

difficult to be reliably measured using traditional GC or GC-MS. Our methods showed significant improvement for the analysis of 7-DHC in control and SLOS plasma samples. **Figure 2A** presents a typical HPLC-MS/MS analysis of a control human blood plasma using the PTAD procedure. Ten microliters of sample from a control volunteer was processed according to the procedures described in Materials and Methods. The levels of free 7-DHC determined for 17 SLOS patients by the PTAD protocol correlate well to the levels determined by GC analysis of the TMS derivative of free 7-DHC, see Fig. 2B.

Under our optimum conditions, analysis of 7-DHC by the PTAD protocol led to a 1,000-fold improvement in the LOD over direct analysis of free 7-DHC by HPLC-APCI-MS/MS. The analysis of 7-DHC-PTAD was carried out with d_7-7-DHC as an internal standard, with the on column LOD being 0.02 pg. Calibration curves for the Des adducts (supplementary Fig. I) show excellent linearity ($r^2 > 0.998$). The relative standard deviation (RSD) for the peak area ratio of each PTAD derivatized compound to the internal standard ranged from 2.5 to 5.8% for intra-vial RSD and from 4.5 to 5.5% for inter-vial RSD, indicating a good precision of the PTAD derivatization method.

The potential for archiving PTAD-derivatized samples for storage and subsequent analysis was investigated by measuring the peak area ratio of each compound compared with the internal standard by LC-MS/MS over an extended

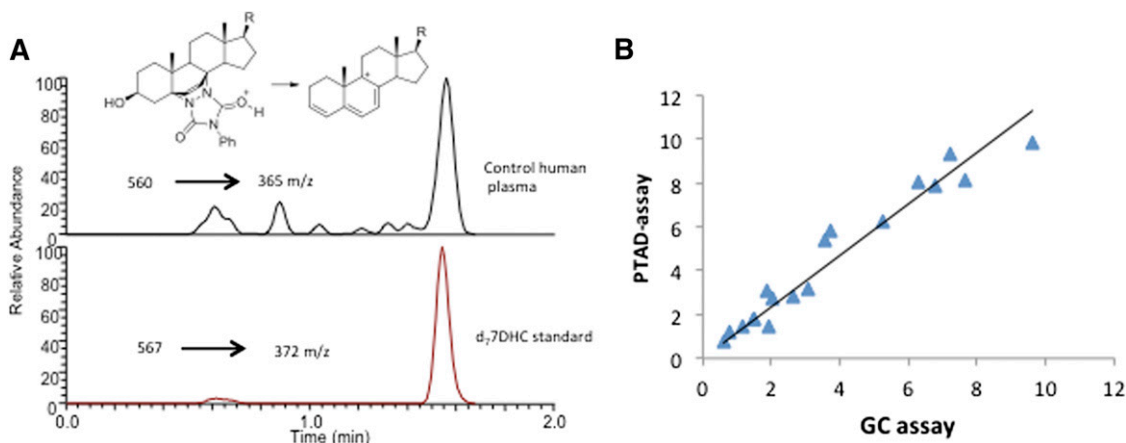**Fig. 2.** A: HPLC-MS/MS assay of 10 µl control human plasma as described in Materials and Methods. B: Correlation of 7-DHC levels in mg/dl for 17 SLOS patients by the PTAD protocol as described in Materials and Methods and a standard GC assay of the 7-DHC TMS derivative. The slope is 1.17 with $r^2 = 0.94$.

time period. The PTAD derivatives of free 7-DHC and free Des gave consistent analytical results after 4 weeks of storage at room temperature in MeOH with no evidence of decomposition or loss of signal strength in the analysis.

7-DHC-PTAD assays in the nervous system of adult WT and SLOS heterozygous mice

Compared with other organs, the brain has a high content of cholesterol. While cholesterol concentration has been measured in numerous reports, 7-DHC concentrations have not been reported previously in the WT mouse nervous system. Therefore, we compared cholesterol and 7-DHC in adult WT and *Dhcr7*-HET mice using the newly developed PTAD assay. We analyzed several brain regions (spinal cord, optic and peripheral nerves, and retina) (see **Table 1** and **Fig. 3**). In all samples, cholesterol and 7-DHC could be reliably determined.

In the adult WT mouse nervous system, the level of cholesterol ranges from 36 ± 12 ng/μg protein in the retina to 393 ± 76 ng/μg protein in the sciatic nerve, with levels of 304 ± 44 ng/μg measured in the brain. In adult HET mice, cholesterol was found to be 29 ± 5 ng/μg protein in the retina, 286 ± 17 ng/μg protein in the sciatic nerve, and 461 ± 80 ng/μg protein in the brain (Table 1). The level of cholesterol in HET mice was significantly increased in the whole brain compared with WT mice ($P < 0.04$). This difference in the whole brain could be accounted for by greatly increased amounts of cholesterol in the cortex, because the other regions do not show statistically significant differences (Fig. 3). 7-DHC levels were more variable than cholesterol, ranging from 5 ± 1 pg/μg protein in the WT retina to 760 ± 140 pg/μg protein in the WT peripheral nerve (Table 1). Notably, 7-DHC levels were greatly increased in all samples in *Dhcr7*-HET mice compared with WT mice, with the highest levels found in the spinal cord ($1,240 \pm 310$ pg/μg protein) and peripheral nerve ($2,560 \pm 500$ pg/μg protein). While both whole brain and spinal cord had somewhat similar levels of cholesterol in WT samples, there was about four times more 7-DHC in the spinal cord than in the whole brain. In *Dhcr7*-HET samples, this difference was even more pronounced with the level of 7-DHC in the spinal cord being eight times higher than in the brain. These differences most likely reflect the difference in the ratio of gray and white matter within the brain and spinal cord.

Because cholesterol biosynthesis peaks during myelination and decreases in the adult brain, we analyzed cholesterol and 7-DHC at two age groups: 2-month- and 7-month-old mice. In the brain at 2 months, cholesterol was increased in *Dhcr7*-HET mice (461 ± 80 ng/μg protein) compared with WT mice (304 ± 44 ng/μg protein). However this difference disappeared over time. At 7 months the cholesterol level decreased in both WT and *Dhcr7*-HET mice and there was no longer a significant difference in the level of cholesterol between the WT and *Dhcr7*-HET brain (177 ± 34 ng/μg protein and 194 ± 30 ng/μg protein, respectively). In contrast, 7-DHC was significantly increased in the Dhcr7-HET brain compared with the WT brain at both 2 and 7 months of age. Thus, at 2 months 7-DHC was 61 ± 13 pg/μg protein for WT and 149 ± 3 pg/μg protein for *Dhcr7*-HET, and at 7 months those values were determined to be 19 ± 3 pg/μg protein and 48 ± 4 pg/μg protein, respectively.

Changes in cholesterol and 7-DHC levels similar to those in the brain were present in peripheral myelin as illustrated by data obtained from the sciatic nerve. While cholesterol was marginally decreased in *Dhcr7*-HET nerves compared with WT nerves at 2 months, even this small difference was not present at 7 months. However, 7-DHC was significantly increased at both time points in *Dhcr7*-HET nerves compared with the controls, at 2 months 7-DHC was 760 ± 140 pg/μg protein for WT and $2,560 \pm 500$ pg/μg protein for HET, and at 7 months 7-DHC was 122 ± 33 pg/μg protein for WT and 360 ± 103 pg/μg protein for HET.

Overall cholesterol biosynthesis decreased in the brain over time, and at 7 months it appeared that there was no difference in cholesterol levels between WT and HET brains. Similarly, the overall 7-DHC level decreased over time in both WT and HET mice, however 7-DHC levels in HET brain were still at significantly higher levels than in WT; therefore, 7-DHC expression does not normalize, but cholesterol does.

7-DHC-PTAD and Des-PTAD assays in the liver and blood of WT and SLOS heterozygous mice

Both 7-DHC and Des were readily detectable in the liver and blood samples of WT and *Dhcr7*-HET mice. A typical chromatogram is shown in **Fig. 4**. The peaks of 7-DHC and d_7-7-DHC-PTAD adducts were observed at 1.51 min in Fig. 4A (m/z 560$\rightarrow$365) and 1.50 min in Fig. 4C (m/z 567$\rightarrow$372), respectively. The Des-PTAD ene product, Des-PTAD, and the PTAD MeOH addition product, Des-PTAD/MeOH, coeluted under the rapid UPLC gradient and they were observed at 1.03 min in both Fig. 4A (m/z 560$\rightarrow$365) and in Fig. 4B (m/z 592$\rightarrow$365). MS and NMR data of these adducts is provided in supplementary Fig. II. The solvent addition product Des-PTAD/MeOH underwent decomposition in the ionization source producing the abundant decomposition ion $[M+H-32]^+$ caused by a loss of MeOH. A characteristic ion fragment with m/z 365 was found in spectra for both the ene and solvent addition products. The

TABLE 1. Cholesterol and 7-DHC distribution in the 8-week-old WT and *Dhcr7*-HET nervous system

	Cholesterol (ng/μg protein)		7-DHC (pg/μg protein)	
	WT	*Dhcr7*-HET	WT	*Dhcr7*-HET
Brain	304 ± 44	461 ± 80	61 ± 13	149 ± 3
Spinal cord	377 ± 88	290 ± 62	270 ± 80	1240 ± 310
Optic nerve	100 ± 27	129 ± 18	20 ± 4	63 ± 11
Peripheral nerve	393 ± 76	286 ± 17	760 ± 140	$2,560 \pm 500$
Retina	36 ± 12	29 ± 5	5 ± 1	8 ± 1

Cholesterol (ng/µg protein)

7-DHC (pg/µg protein)
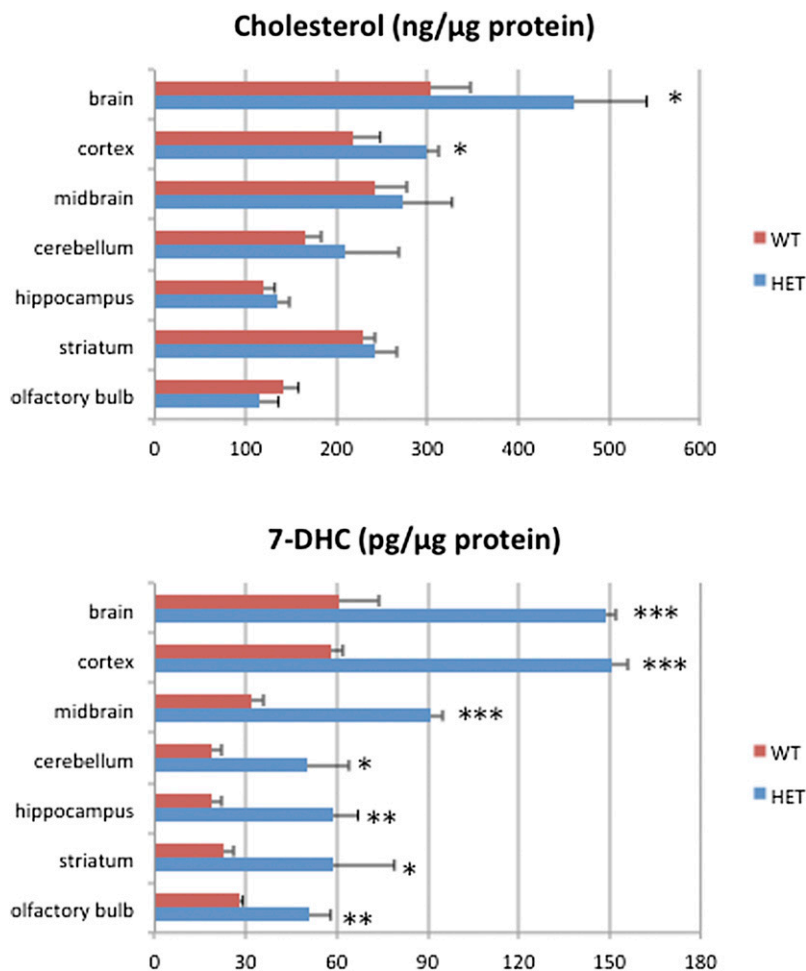
Fig. 3. Regional cholesterol and 7-DHC distribution in 8-week-old WT and *Dhcr7*-HET mouse brains. Data are expressed as mean values ± SD. *$P < 0.05$, **$P < 0.005$, ***$P < 0.001$, as compared with the WT mice.

$[M+H]^+$ ion was the dominant ion formed for each adduct and was used as parent in the SRM protocol in each case.

The PTAD method improves the sensitivity and speed of Des analysis as shown here and the method should find general utility for sterols containing the Δ24-25 double bond. A more complete analysis of several important sterols by the PTAD method is under investigation in the tissues and blood of *Dhcr7*- or *Dhcr24*-HET and -KO mice and the results of these investigations will be reported in due course. The method also offers the potential to screen the blood of human carriers of *DHCR7* and *DHCR24* mutations.

7-DHC-PTAD assays in cell cultures

As a final demonstration of the PTAD assay we report on the use of the method to determine 7-DHC in cultures of control and *Dhcr7*-deficient Neuro2a cells. The comparison of control Neuro2a, *Dhcr7*-deficient Neuro2a, and Neuro2a cells treated with increasing concentrations of AY9944, a known inhibitor of DHCR7, is shown in **Table 2** (32–34). Control Neuro2a cells had very little 7-DHC while *Dhcr7*-deficient Neuro2a cells had greatly increased 7-DHC accumulation. In AY9944-treated Neuro2a cells, there was a dose-response increase in 7-DHC levels and 50 nM of AY9944 gave similar levels of 7-DHC as seen in *Dhcr7*-deficient Neuro2a cells. To determine the sensitivity of the assay, we measured 7-DHC in a specified number of control Neuro2a and *Dhcr7*-deficient Neuro2a cells (supplementary Table I and

supplementary Fig. III). We found that 7-DHC could be reliably measured in about 5,000 control cells and Des in about 125 control cells. The correlation of 7-DHC with number of cells for *Dhcr7*-deficient Neuro2a cells is defined by the equations: 7-DHC (ng) = 2.645 (cell number/1,000) with $r^2 = 0.98$; and the value for Des was Des (ng) = 0.2579 (cell number/1,000) with $r^2 = 0.99$. For WT Neuro2a cells, the correlation equations for 7-DHC and Des are: 7-DHC (ng) = 0.0078 (cell number/1,000) with $r^2 = 0.94$ and Des (ng) = 1.4186 (cell number/1,000) with $r^2 = 0.97$. These data show that the PTAD method should be applicable to 7-DHC measurements in a single well of a 96-well plate.

DISCUSSION

Advances in lipid biology have been accelerated by powerful analytical techniques, principal among these being the use of HPLC-MS. Electrospray ionization (ESI) and APCI-MS methods coupled with HPLC and the use of deuterated lipid standards have played an essential role in recent advances in lipidomics. The Lipid Maps Consortium in particular, has made good use of these techniques to define the important lipid classes and molecular species in a variety of biological fluids, cells, and tissues (35–37). Methods for analysis of many sterols and oxysterols that rely on HPLC-MS have been reported that are exquisitely sensitive
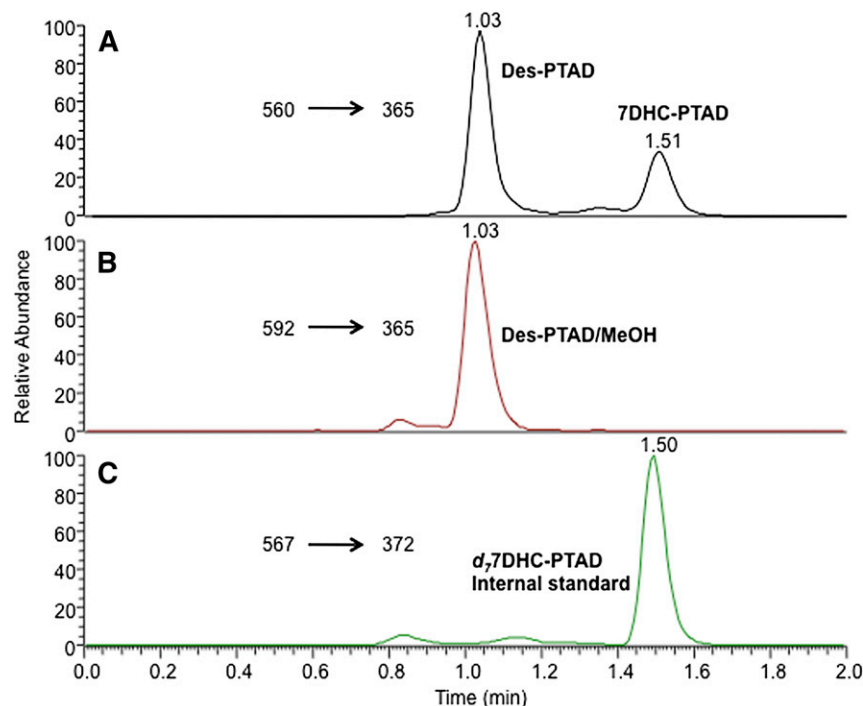
Fig. 4. HPLC-MS analysis of liver tissue from a 2-month-old WT mouse using the PTAD analysis method as described in Materials and Methods. Des was analyzed at 1.77 ± 0.50 ng/mg tissue in the adult WT mouse liver while 7-DHC was determined to be 0.20 ± 0.05 ng/mg tissue.

and convenient (36, 38–43), the recent work of Griffiths and colleagues (38–42) being particularly noteworthy. 7-DHC poses particular problems for analysis because it undergoes free radical chain oxidation readily. Analysis of 7-DHC in biological tissues and fluids can therefore be subject to large variability due to different conditions of sample storage (44). Indeed, 7-DHC is one of the most reactive organic molecules known in free radical chain oxidation reactions, and samples containing this sterol may be compromised if appropriate care is not taken in sample collection and storage. The addition of the antioxidant BHT and the peroxide reducing agent TPP to samples as soon as possible offers some stabilization, but conversion of the conjugated diene to a more stable functionality by reaction with PTAD provides further protection (44, 45).

7-DHC is a prototypical Diels-Alder diene and PTAD is one of the most reactive Diels-Alder dienophiles known. Indeed, the Diels-Alder adducts of PTAD and sterol ring B dienes, such as ergosterol and 7-DHC, have been known for over 40 years (46–48). The PTAD adduct of 7-DHC has also been

used in synthetic transformations as a protecting group for the reactive diene substructure (47). The studies reported here confirm the reactivity of 7-DHC and PTAD and demonstrate that the Diels-Alder adduct is well-behaved on HPLC and is readily detected by MS. Perhaps equally important is the fact that the conjugated diene in the sterol ring B is stabilized toward oxidation by reaction with PTAD making biological samples suitable for subsequent storage or shipment and analysis. Thus, acquisition of plasma samples by methods that minimize peroxidation during collection (44, 45) followed by a workup that includes reaction with PTAD gives samples that are suitable for archival purposes. The workup is a simple modification of the Folch method that does not require specialized equipment, the reagents are readily available and the chromatographic run is less than 5 min.

An added benefit of the PTAD method is the fact that Des is also derivatized by an ene reaction with PTAD under the standard conditions of workup (29). The Des-PTAD adducts (Des-PTAD and Des-PTAD/MeOH) readily separate from the 7-DHC-PTAD product by HPLC, and

TABLE 2. Cholesterol and 7-DHC in control Neuro2a, *Dhcr7*-deficient Neuro2a, and Neuro2a cells treated with increasing concentrations of AY9944, a known inhibitor of DHCR7

Neuro 2a	Cholesterol (ng/µg protein)	7-DHC (ng/µg protein)	7-DHC/Cholesterol Ratio
Dhcr7-deficient	31.5 ± 6.3	33.3 ± 6.2	1.07 ± 0.21
Control	31.3 ± 5.4	0.21 ± 0.01	0.007 ± 0.001
Control + AY9944 (1 nM)	30.5 ± 4.1	1.39 ± 0.09	0.046 ± 0.003
Control + AY9944 (10 nM)	27.5 ± 2.2	21.5 ± 5.1	0.78 ± 0.17
Control + AY9944 (50 nM)	14.4 ± 3.7	25.4 ± 4.2	1.80 ± 0.36

For AY9944 treatment Neuro2a cells were plated at $5 \times 10^4/cm^2$ in DMEM with 10% FBS. The following day medium was replaced with serum-free medium (DMEM plus N2 supplement) with different AY9944 concentrations (1 nM, 10 nM, and 50 nM) for 48 h.

adducts of the two sterols can be readily distinguished by SRM in HPLC-MS. In MeOH, the isolated alkene at C24 of Des is apparently more reactive with PTAD than the ring B olefins present in that sterol or the similar alkene present in cholesterol. Thus, a MeOH-PTAD workup of samples containing cholesterol, Des, and 7-DHC provides an assay for both 7-DHC and Des without any complication by the presence of cholesterol, which is normally present at much higher levels than 7-DHC or Des. The on-column LOD of 0.02 pg makes the assay appropriate for analysis of cells in culture as well as biological tissues and fluids.

Our previous studies of the mouse SLOS model ($Dhcr7^{tm1Gst}$-KO mice) showed that almost all of the cholesterol in the brain of the P0 KO mouse was replaced by 7-DHC (13, 15). 7-DHC was not detected in WT samples because it was below the detection limit of the GC system used, which is also in agreement with previous studies of sterols in the brain (49). Because $Dhcr7^{tm1Gst}$-KO mice die shortly after birth and very little 7-DHC is found throughout developing and adult WT mouse brain, using the PTAD assay, we designed experiments to compare 7-DHC and cholesterol in the adult WT and $Dhcr7$-HET mouse samples with this new method. We found that 7-DHC was present at 1,000–10,000 lower levels than cholesterol: while cholesterol was measured in ng/µg protein, 7-DHC was measured in pg/µg protein. Within the WT nervous system, specific brain regions had greater variability in the levels of 7-DHC than in the levels of cholesterol, most likely reflecting the difference in the expression of cholesterol biosynthesis enzymes or differences in the regulation of cholesterol biosynthesis.

In adult $Dhcr7$-HET mice, 7-DHC was increased about two times compared with WT samples. The smallest increase of 7-DHC was in the retina and the largest increase was in the spinal cord. In addition to changes in neuronal 7-DHC levels, we found significant increases in both the central and peripheral myelin of $Dhcr7$-HET compared with WT mice. Because, for the most part, $Dhcr7$-HET mice appear indistinguishable from WT mice, behavioral testing was undertaken to ascertain if there are basal behavioral differences between $Dhcr7$-HET and WT mice (50). $Dhcr7$-HET mice did not differ from WT mice on basic measures of locomotor activity, anxiety, and neuromuscular ability. However, female $Dhcr7$-HET mice at 6 months of age or older were significantly more likely to win on the social dominance tube test against an unfamiliar mouse. Pharmacological testing, using the 5-HT2A agonist, 1-(2,5-dimethoxy-4-iodophenyl)-2-aminopropane, showed increased head-twitch response in $Dhcr7$-HET mice, which was apparent from 6 months of age. Based on these studies, it was suggested that the chronic accumulation of 7-DHC or 7-DHC-derived oxysterols in the HET nervous system may increase oxidative stress and underlie some of the behavioral changes observed in these mice (50).

Two questions of potential interest are: what is the minimum amount of 7-DHC accumulation required for manifestations of pathology and are HET carriers vulnerable? It is of some interest that carriers of another autosomal recessive disorder, cystic fibrosis, appear to be more vulnerable to lung disorders and the related environmental stresses. In particular, they appear to have a higher incidence of increased lung airway reactivity and its associated symptoms and an elevated risk for poor pulmonary function, including asthma (51, 52). While haploinsufficiency of the DHCR7 enzyme in HET carriers has not been associated with pathology, 7-DHC determination is not a generally common assay of the general population. The sensitive assay for 7-DHC in tissues and fluids reported here provides a rapid means to identify samples having elevated levels of this reactive species, regardless of whether the cause of the increase is genetic or environmental (18, 19, 53).

While 7-DHC accumulates in the $Dhcr7$-HET liver, the overall load is more pronounced in the brain. Blood 7-DHC measurements reflect biosynthesis in the liver and although differences in 7-DHC blood levels between WT and $Dhcr7$-HET mice are not significant, there are significant changes in the nervous system. Therefore the measurement of 7-DHC within blood may not reflect fully the severity present in the nervous system.

We suggest that the PTAD method reported here presents a useful alternative for the analysis of 7-DHC and Des. These two compounds in the sterol pathway are receiving increased attention because of their critical position as immediate precursors of cholesterol. Rapid and reliable screening of biological tissues, fluids, and cells for 7-DHC and Des at typically "normal" or "control" levels is now reasonably straightforward with the PTAD method. While the ring B alkene of cholesterol at Δ5-6 has little or no reactivity as a PTAD ene reaction partner, sterols with alkenes located at other ring sites (Δ7-6 or Δ8-9) may show greater reactivity and provide pathways for derivatization that prove useful. We note that biological samples that have elevated 7-DHC usually also have elevated 8-DHC and the PTAD protocol has not yet provided a clean assay for this isomer. At a minimum, the approach provides a sensitive and rapid first screen to identify samples that have a distorted sterol profile and studies that make use of and extend the protocol to other sterols are ongoing.⬛

REFERENCES

1. Dietschy, J. M., and S. D. Turley. 2001. Cholesterol metabolism in the brain. *Curr. Opin. Lipidol.* **12:** 105–112.
2. Nes, W. D. 2011. Biosynthesis of cholesterol and other sterols. *Chem. Rev.* **111:** 6423–6451.
3. Heverin, M., N. Bogdanovic, D. Lutjohann, T. Bayer, I. Pikuleva, L. Bretillon, U. Diczfalusy, B. Winblad, and I. Bjorkhem. 2004. Changes in the levels of cerebral and extracerebral sterols in the brain of patients with Alzheimer's disease. *J. Lipid Res.* **45:** 186–193.
4. Porter, F. D., and G. E. Herman. 2011. Malformation syndromes caused by disorders of cholesterol synthesis. *J. Lipid Res.* **52:** 6–34.
5. Smith, D. W., L. Lemli, and J. M. Opitz. 1964. A newly recognized syndrome of multiple congenital anomalies. *J. Pediatr.* **64:** 210–217.
6. Irons, M., E. R. Elias, G. Salen, G. S. Tint, and A. K. Batta. 1993. Defective cholesterol biosynthesis in Smith-Lemli-Opitz syndrome. *Lancet.* **341:** 1414.
7. Kelley, R. I., and R. C. M. Hennekam. 2000. The Smith-Lemli-Opitz syndrome. *J. Med. Genet.* **37:** 321–335.
8. Porter, F. D. 2003. Human malformation syndromes due to inborn errors of cholesterol synthesis. *Curr. Opin. Pediatr.* **15:** 607–613.
9. Fitzky, B. U., F. F. Moebius, H. Asaoka, H. Waage-Baudet, L. Xu, G. Xu, N. Maeda, K. Kluckman, S. Hiller, H. Yu, et al. 2001. 7-Dehydrocholesterol-dependent proteolysis of HMG-CoA reductase suppresses sterol biosynthesis in a mouse model of Smith-Lemli-Opitz/RSH syndrome. *J. Clin. Invest.* **108:** 905–915.

10. Schaaf, C. P., J. Koster, P. Katsonis, L. Kratz, O. A. Shchelochkov, F. Scaglia, R. I. Kelley, O. Lichtarge, H. R. Waterham, and M. Shinawi. 2011. Desmosterolosis-phenotypic and molecular characterization of a third case and review of the literature. *Am. J. Med. Genet. A.* **155A:** 1597–1604.

11. Xu, L., T. A. Davis, and N. A. Porter. 2009. Rate constants for peroxidation of polyunsaturated fatty acids and sterols in solution and in liposomes. *J. Am. Chem. Soc.* **131:** 13037–13044.

12. Xu, L., Z. Korade, and N. A. Porter. 2010. Oxysterols from free radical chain oxidation of 7-dehydrocholesterol: product and mechanistic studies. *J. Am. Chem. Soc.* **132:** 2222–2232.

13. Xu, L., Z. Korade, D. A. Rosado, W. Liu, C. R. Lamberson, and N. A. Porter. 2011. An oxysterol biomarker for 7-dehydrocholesterol oxidation in cell/mouse models for Smith-Lemli-Opitz syndrome. *J. Lipid Res.* **52:** 1222–1233.

14. Xu, L., W. Liu, L. G. Sheflin, S. J. Fliesler, and N. A. Porter. 2011. Novel oxysterols observed in tissues and fluids of AY9944-treated rats: a model for Smith-Lemli-Opitz syndrome. *J. Lipid Res.* **52:** 1810–1820.

15. Korade, Z., L. Xu, K. Mirnics, and N. A. Porter. 2013. Lipid biomarkers of oxidative stress in a genetic mouse model of Smith-Lemli-Opitz syndrome. *J. Inherit. Metab. Dis.* **36:** 113–122.

16. Korade, Z., L. Xu, R. Shelton, and N. A. Porter. 2010. Biological activities of 7-dehydrocholesterol-derived oxysterols: implications for Smith-Lemli-Opitz syndrome. *J. Lipid Res.* **51:** 3259–3269.

17. Xu, L., K. Mirnics, A. B. Bowman, W. Liu, J. Da, N. A. Porter, and Z. Korade. 2012. DHCEO accumulation is a critical mediator of pathophysiology in a Smith-Lemli-Opitz syndrome model. *Neurobiol. Dis.* **45:** 923–929.

18. Canfrán-Duque, A., M. E. Casado, O. Pastor, J. Sánchez-Wandelmer, G. de la Peña, M. Lerma, P. Mariscal, F. Bracher, M. A. Lasunción, and R. Busto. 2013. Atypical antipsychotics alter cholesterol and fatty acid metabolism in vitro. *J. Lipid Res.* **54:** 310–324.

19. Hall, P., V. Michels, D. Gavrilov, D. Matern, D. Oglesbee, K. Raymond, P. Rinaldo, and S. Tortorelli. 2013. Aripiprazole and trazodone cause elevations of 7-dehydrocholesterol in the absence of Smith-Lemli-Opitz syndrome. *Mol. Genet. Metab.* **110:** 176–178.

20. Higashi, T., K. Shimada, and T. Toyo'oka. 2010. Advances in determination of vitamin D related compounds in biological samples using liquid chromatography-mass spectrometry: a review. *J. Chromatogr. B Analyt. Technol. Biomed. Life Sci.* **878:** 1654–1661.

21. Alberti, M. N., and M. Orfanopoulos. 2009. Concerning the reactivity of PTAD with isomeric dienes: the mechanism of the Diels-Alder cycloaddition. *Org. Lett.* **11:** 1659–1662.

22. Roubelakis, M. M., G. C. Vougioukalakis, Y. S. Angelis, and M. Orfanopoulos. 2006. Solvent-dependent changes in the ene reaction of RTAD with alkenes: the cyclopropyl group as a mechanistic probe. *Org. Lett.* **8:** 39–42.

23. Vougioukalakis, G. C., and M. Orfanopoulos. 2005. Mechanistic studies in triazolinedione ene reactions. *Synlett.* **5:** 713–731.

24. Vougioukalakis, G. C., M. M. Roubelakis, M. N. Alberti, and M. Orfanopoulos. 2008. Solvent-dependent changes in the triazolinedione-alkene ene reaction mechanism. *Chemistry.* **14:** 9697–9705.

25. Acevedo, O., and M. E. Squillacote. 2008. A new solvent-dependent mechanism for a triazolinedione ene reaction. *J. Org. Chem.* **73:** 912–922.

26. Anastasia, M., A. Fiecchi, and G. Galli. 1981. Synthesis of cholesta-5,8-dien-3-beta-ol. *J. Org. Chem.* **46:** 3421–3422.

27. Wolf, C., F. Chevy, J. Pham, M. Kolf-Clauw, D. Citadelle, N. Mulliez, and C. Roux. 1996. Changes in serum sterols of rats treated with 7-dehydrocholesterol-delta 7-reductase inhibitors: comparison to levels in humans with Smith-Lemli-Opitz syndrome. *J. Lipid Res.* **37:** 1325–1333.

28. Korade, Z., A. K. Kenworthy, and K. Mirnics. 2009. Molecular consequences of altered neuronal cholesterol biosynthesis. *J. Neurosci. Res.* **87:** 866–875.

29. Elemes, Y., and M. Orfanopoulos. 1991. Triazolinedione additions to alkenes in protic solvents. A remarkable temperature dependence of the competing reaction paths. *Tetrahedron Lett.* **32:** 2667–2670.

30. Patrono, C., C. Rizzo, A. Tessa, A. Giannotti, P. Borrelli, R. Carrozzo, F. Piemonte, E. Bertini, C. Dionisi-Vici, and F. M. Santorelli. 2000. Novel 7-DHCR mutation in a child with Smith-Lemli-Opitz syndrome. *Am. J. Med. Genet.* **91:** 138–140.

31. Kelley, R. I. 1995. Diagnosis of Smith-Lemli-Opitz syndrome by gas chromatography/mass spectrometry of 7-dehydrocholesterol in plasma, amniotic fluid and cultured skin fibroblasts. *Clin. Chim. Acta.* **236:** 45–58.

32. Richards, M. J., B. A. Nagel, and S. J. Fliesler. 2006. Lipid hydroperoxide formation in the retina: correlation with retinal degeneration and light damage in a rat model of Smith-Lemli-Opitz syndrome. *Exp. Eye Res.* **82:** 538–541.

33. Suzuki, K., and L. D. De Paul. 1971. Cellular degeneration in developing central nervous system of rats produced by hypocholesteremic drug AY9944. *Lab. Invest.* **25:** 546–555.

34. Keller, R. K., D. A. Mitchell, C. C. Goulah, and S. J. Fliesler. 2013. Hepatic isoprenoid metabolism in a rat model of Smith-Lemli-Opitz syndrome. *Lipids.* **48:** 219–229.

35. Quehenberger, O., A. M. Armando, A. H. Brown, S. B. Milne, D. S. Myers, A. H. Merrill, S. Bandyopadhyay, K. N. Jones, S. Kelly, R. L. Shaner, et al. 2010. Lipidomics reveals a remarkable diversity of lipids in human plasma. *J. Lipid Res.* **51:** 3299–3305.

36. McDonald, J. G., D. D. Smith, A. R. Stiles, and D. W. Russell. 2012. A comprehensive method for extraction and quantitative analysis of sterols and secosteroids from human plasma. *J. Lipid Res.* **53:** 1399–1409.

37. Milne, S., P. Ivanova, J. Forrester, and H. Alex Brown. 2006. Lipidomics: an analysis of cellular lipids by ESI-MS. *Methods.* **39:** 92–103.

38. Griffiths, W. J., Y. Wang, G. Alvelius, S. Liu, K. Bodin, and J. Sjovall. 2006. Analysis of oxysterols by electrospray tandem mass spectrometry. *J. Am. Soc. Mass Spectrom.* **17:** 341–362.

39. Griffiths, W. J., Y. Wang, K. Karu, E. Samuel, S. McDonnell, M. Hornshaw, and C. Shackleton. 2008. Potential of sterol analysis by liquid chromatography-tandem mass spectrometry for the prenatal diagnosis of Smith-Lemli-Opitz syndrome. *Clin. Chem.* **54:** 1317–1324.

40. Griffiths, W. J., M. Hornshaw, G. Woffendin, S. F. Baker, A. Lockhart, S. Heidelberger, M. Gustafsson, J. Sjövall, and Y. Wang. 2008. Discovering oxysterols in plasma: a window on the metabolome. *J. Proteome Res.* **7:** 3602–3612.

41. Griffiths, W. J., A. Brown, R. Reimendal, Y. Yang, J. Zhang, and J. Sjövall. 1996. A comparison of fast-atom bombardment and electrospray as methods of ionization in the study of sulphated- and sulphonated-lipids by tandem mass spectrometry. *Rapid Commun. Mass Spectrom.* **10:** 1169–1174.

42. Meljon, A., G. L. Watson, Y. Wang, C. H. Shackleton, and W. J. Griffiths. 2013. Analysis by liquid chromatography-mass spectrometry of sterols and oxysterols in brain of the newborn Dhcr7(Δ3-5/T93M) mouse: a model of Smith-Lemli-Opitz syndrome. *Biochem. Pharmacol.* **86:** 43–55.

43. Honda, A., K. Yamashita, H. Miyazaki, M. Shirai, T. Ikegami, G. Xu, M. Numazawa, T. Hara, and Y. Matsuzaki. 2008. Highly sensitive analysis of sterol profiles in human serum by LC-ESI-MS/MS. *J. Lipid Res.* **49:** 2063–2073.

44. Liu, W., L. Xu, C. Lamberson, L. Merkens, R. Steiner, E. Elias, D. Haas, and N. Porter. 2013. Assays of plasma dehydrocholesteryl esters and oxysterols from Smith-Lemli-Opitz syndrome patients. *J. Lipid Res.* **54:** 244–253.

45. Liu, W., H. Yin, Y. O. Akazawa, Y. Yoshida, E. Niki, and N. A. Porter. 2010. Ex vivo oxidation in tissue and plasma assays of hydroxyoctadecadienoates: Z,E/E,E stereoisomer ratios. *Chem. Res. Toxicol.* **23:** 986–995.

46. Barton, D. H. R., T. Shioiri, and D. A. Widdowson. 1971. Biosynthesis of terpenes and steroids. Part V. The synthesis of ergosta-5,7,22,24(28)-tetraen-3β-ol, a biosynthetic precursor of ergosterol. *J. Chem. Soc. C.* **1971:** 1968–1974.

47. Kim, H. S., W. K. Wilson, D. H. Needleman, F. D. Pinkerton, D. K. Wilson, F. A. Quiocho, and G. J. Schroepfer. 1989. Inhibitors of sterol synthesis. Chemical synthesis, structure, and biological activities of (25R)-3β,26-dihydroxy-5α-cholest-8(14)-en-15-one, a metabolite of 3β-hydroxy-5α-cholest-8(14)-en-15-one. *J. Lipid Res.* **30:** 247–261.

48. Johnson, D. W., H. J. ten Brink, and C. Jakobs. 2001. A rapid screening procedure for cholesterol and dehydrocholesterol by electrospray ionization tandem mass spectrometry. *J. Lipid Res.* **42:** 1699–1705.

49. Tint, G. S., H. Yu, Q. Shang, G. Xu, and S. B. Patel. 2006. The use of the Dhcr7 knockout mouse to accurately determine the origin of fetal sterols. *J. Lipid Res.* **47:** 1535–1541.

50. Korade, Z., O. M. Folkes, and F. E. Harrison. 2013. Behavioral and serotonergic response changes in the Dhcr7-HET mouse model of Smith-Lemli-Opitz syndrome. *Pharmacol. Biochem. Behav.* **106:** 101–108.

51. Davis, P. B., and K. Vargo. 1987. Pulmonary abnormalities in obligate heterozygotes for cystic fibrosis. *Thorax.* **42:** 120–125.

52. Dahl, M., A. Tybjaerg-Hansen, P. Lange, and B. G. Nordestgaard. 1998. DeltaF508 heterozygosity in cystic fibrosis and susceptibility to asthma. *Lancet.* **351:** 1911–1913.

53. Hall, P., V. Michels, D. Gavrilov, D. Matern, D. Oglesbee, K. Raymond, P. Rinaldo, and S. Tortorelli. 2013. Aripiprazole and trazodone cause elevations of 7-dehydrocholesterol in the absence of Smith-Lemli-Opitz Syndrome. *Mol. Genet. Metab.* **110:** 176–178.